

# A SIMULATION-BASED OPTIMIZATION OF THE SECONDARY LOOP OF GENTILLY-2 NUCLEAR POWER PLANT

J. Dipama<sup>1</sup>, W. Hounkonnou<sup>1</sup>, A. Teyssedou<sup>1\*</sup> & F. Aubé<sup>2</sup>  
<sup>1</sup>Nuclear Engineering Institute, Engineering Physics Department  
École Polytechnique de Montréal,  
Québec, CANADA

<sup>2</sup>CANMET Energy Diversification Research Laboratory  
Varenes, Québec, CANADA

## Abstract

Increasing the thermodynamic efficiency of fossil fuel or nuclear power plants can lead to significant economic gains. Consequently, the continuous quest of searching higher efficiency in power plants has resulted in the development of innovative tools to comply with these needs. Although a large inventory of simulation tools is available for industrial applications, sometimes it is more appropriate to develop in-house models that are more suitable for treating specific energy systems. In the present work, a combined simulation-optimization tool was developed and used to optimize the secondary loop of the Gentilly-2 nuclear power plant. Based on previous studies [1] the optimizer module has been now coupled with a thermodynamic model, written in Matlab, used as a plant simulation tool. It includes models that take into account the responses of major thermal units, i.e., condenser, moisture separator reheater (MSR) and feedwater heaters. The simulation package is used to estimate the behavior of the power station according to the variation of a given number of plant-operation parameters. The proposed methodology permits a set of better trade-off operating conditions of the secondary loop to be determined, and thus providing a better and more realistic support to plant operators. The results also clearly show that there is plenty of potential to improve the overall performance of the power station.

*Keywords:* CANDU reactor, thermodynamic cycle, nuclear power plant, multi-objective optimization, evolutionary algorithms, Pareto's front.

---

\* Corresponding author: A. Teyssedou, e-mail [alberto.teyssedou@polymtl.ca](mailto:alberto.teyssedou@polymtl.ca)

## 1. Introduction

In a pressurized water nuclear reactor such as CANDU ones, close to saturation steam is used at the entrance of the high-pressure (HP) turbine that leads to an increase of its humidity content (i.e., formation of liquid droplets) when it expands through the stages. The formation of liquid droplets tends to deteriorate both the turbine's integrity (i.e., increases the erosion of the blades) as well as its efficiency. If a small amount of humidity is tolerated at the outlet of the last HP stage, a vapor superheating is necessary before it enters into the low-pressure (LP) unit. Lior [2] studied the effect of superheating steam in nuclear power plants before entering into a LP turbine, by using an auxiliary external fossil fuel source. He stated that superheating makes it possible to increase the generated power by about 70% and the cycle efficiency by 16%. In CANDU power plants, an external heat source is not used; instead, the required superheating is obtained by a derivation of a fraction of the steam produced in the steam generators (SGs) as shown in Figure 1. Thus, for a given amount of generated steam, this flow redistribution may increase the available energy at the entrance of the LP turbine but it reduces the total work produced by the HP unit. The problem that rises then is to estimate how much steam must be derived in order to ensure better trade-off between turbine efficiency and mechanical work.

Moreover, most modern thermal power plants regenerate part of the thermal energy in feedwater heaters before closing the thermodynamic cycle. A practical regeneration process is accomplished by extracting steam from the turbine at various points to heat the feedwater before its return to the steam generators. The problem that rises in this operation is the determination of the optimal fractions of steam to be extracted at different stages of the turbine that will permit operating conditions that realize the best compromise between the overall cycle efficiency and the power produced by the plant to be achieved [3].

Combining reheat and regeneration in an optimal way, to improve simultaneously the output power and the overall plant efficiency is the main purpose of this study. It constitutes a complex multi-objective optimization problem that requires convenient modeling tools. The results can help both designers and operators to make a more convenient selection of the plant operation parameters. Conventional optimization approaches (e.g., gradient methods) used in the past to solve very simple problems are not suitable for handling multi-objective optimization problems. In the last decades, new approaches including evolutionary algorithms have been used to provide reliable solutions of complex systems [4]. Evolutionary algorithms (EAs) have been successfully applied to a cogeneration system having two objective functions [5]. Recently, EAs have also been used for synthesizing complex heat exchangers networks [6]. The present study is a continuation of previous work carried out in this area and given in reference [1]. In turn, the present paper presents a combined simulation-optimization approach based on evolutionary algorithms to determine optimal operation conditions of the secondary loop of Gentilly-2 nuclear power plant, which includes modeling of major thermal equipments. Thus, the optimizer is coupled with a thermodynamic plant-model written in Matlab that is able to take into account the responses of each thermal unit such as the condenser, feedwater heaters, moisture separator reheater and deaerator. Coupling the plant simulator and the optimizer modules allows optimization parameters to be considered as independent variables that can be freely changed within certain margins. This procedure permits the optimizer to determine the best state variables, which satisfy specified objective functions.

## 2. Thermodynamic simulation model

The optimization of a power station necessitates previous results obtained from simulations of the system considered as a whole; therefore, it is important to develop accurate models capable to handle different thermal units encountered in the plant. Figure 1 shows the flowsheet of the secondary loop of Gentilly-2 nuclear power plant. It consists of a conventional reheat-regenerative Rankine cycle with high-pressure (HP) and low-pressure (LP) turbines running in tandem. The thermodynamic states of the cycle are shown by open circles with numbers, while the thermal equipments are identified using their engineering technical designations.

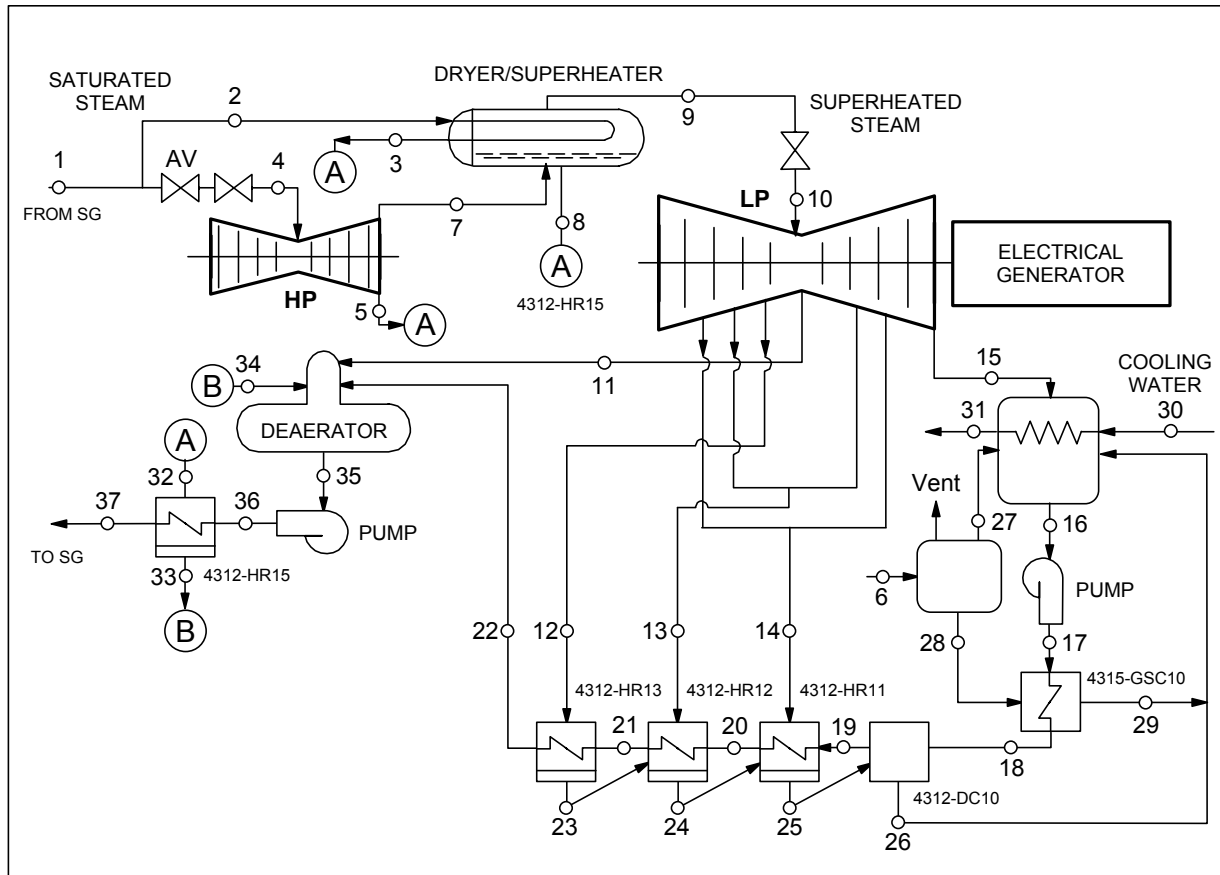


Figure 1 Schematic of Gentilly-2 secondary loop.

### 2.1 The turbine

A turbine is composed by series of stages constituted by rows of fixed nozzles and moving blades. The thermal efficiency of steam turbines can be estimated from empirical relationships that require various turbine geometrical and characteristic parameters. Stodola [7] developed a semi-analytical approach (i.e., Stodola's ellipse) to predict the turbine performance under both design and off-design conditions. Thus, the turbine is divided into multistage groups (see Figure 2) according to steam extraction points and each group is treated as a single nozzle system. Stodola's ellipse law states that the vapor mass flow rate along each group can be determined as:

$$\dot{m}_k = C_k \mathbf{p}_k \sqrt{\frac{P_k}{\mathbf{u}_k}}, \quad (1)$$

where  $P_k$  and  $\mathbf{u}_k$  are the pressure and the specific volume at the entrance of the group, respectively and  $C_k$  is the Stodola's ellipse constant. The parameter  $\mathbf{p}_k$  is the ellipse factor and is expressed as follows:

$$\mathbf{p}_k = \sqrt{1 - \left(\frac{P_{k-1}}{P_k}\right)^2}, \quad (2)$$

where  $P_{k-1}$  is the pressure at the exit of the extraction for group  $k$ , as shown in Figure 2.

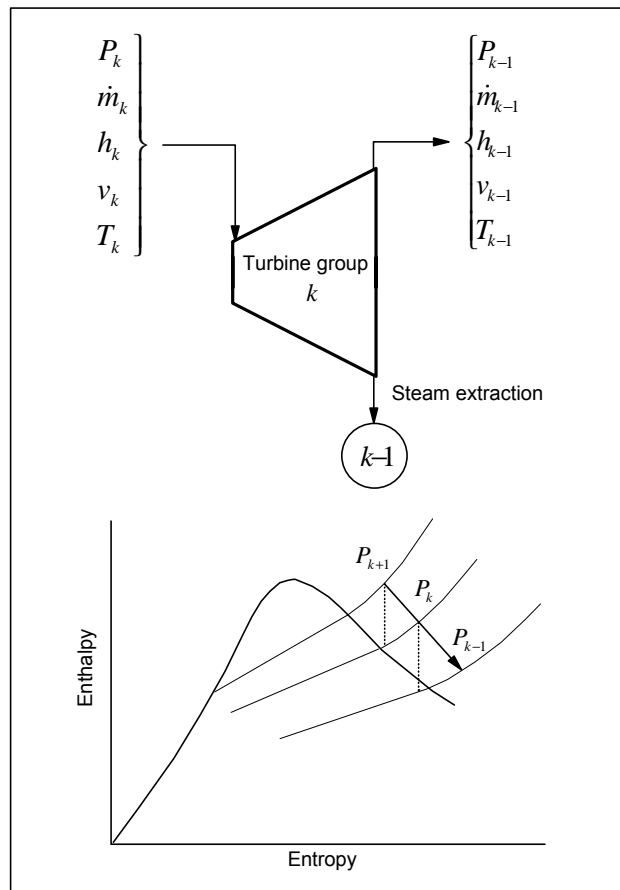


Figure 2 Multistage turbine group [7].

Although the use of Equations (1) and (2) can help to tackle some turbine problems, their application is not always easy because of the unavailability of all the data necessary to perform the calculations. Therefore, in this work it is assumed that the efficiency of each group is constant and it corresponds to the value determined from the actual operating conditions of the power plant. Consequently, the pressures at different extraction points of the turbine are not linked to possible pressure losses, therefore they are determined from the conditions prevailing in the shell-side of the corresponding feedwater heater.

## 2.2 The moisture separator reheater (MSR) system

Since in the nuclear power plant steam is not superheated, it may contain a considerable amount of moisture in most of turbine stages. Erosion resulting from the presence of droplets can have a serious negative impact on the mechanical integrity of the turbine, reducing its overall efficiency. Therefore, the moisture separator-reheater (see Figure 1) is used to improve the thermal efficiency of the power plant and to reduce the mechanical losses in the low-pressure turbine. Wetted steam at the exhaust of the HP turbine flows through chevrons that collect the moisture, mechanically drying the vapor and draining out the droplets. Figure 3 shows a simplified schematic of this unit. It can be analyzed from simple energy and mass balances, which yield:

$$\dot{m}_2 h_2 + \dot{m}_9 h_9 - \dot{m}_3 h_3 - \dot{m}_{10} h_{10} = 0, \quad (3)$$

$$\dot{m}_3 = \dot{m}_2, \quad (4)$$

$$\dot{m}_{10} = \dot{m}_9, \quad (5)$$

$$\dot{m}_2 (h_2 - h_3) = \dot{m}_9 (h_9 - h_{10}). \quad (6)$$

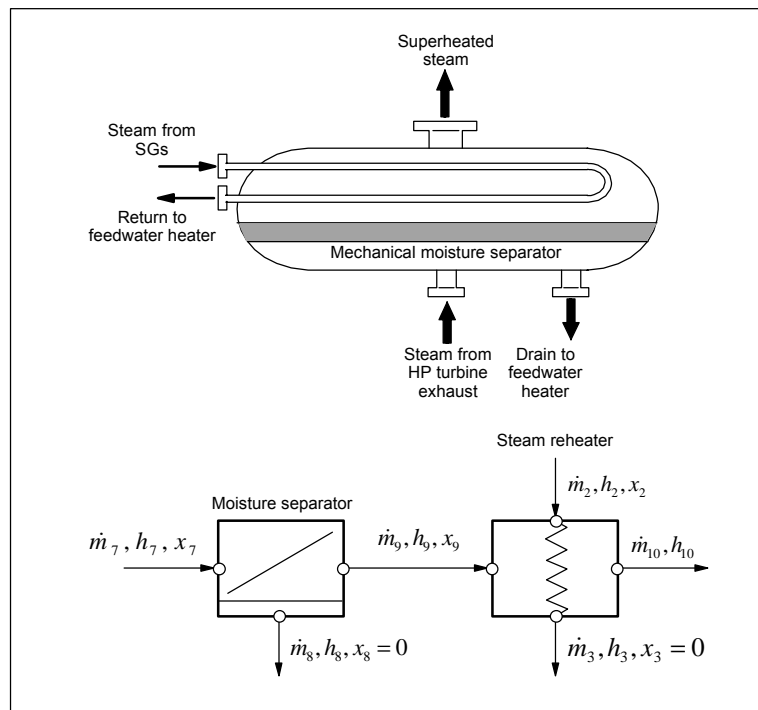


Figure 3 Moisture separator-reheater system.

Assuming a complete separation of moisture (i.e.,  $x_9 = 1$ ), the steam mass flow rate ( $\dot{m}_9$ ) is calculated as:

$$x_7 = \frac{\dot{m}_9}{\dot{m}_7}, \quad (7)$$

and the condensate mass flow rate becomes:

$$\dot{m}_8 = \dot{m}_7(1 - x_7). \quad (8)$$

The thermodynamic properties of the steam at state 9 (see Figure 1) are determined based on the value of the steam quality ( $x_9 = 1$ ) and the pressure ( $P_9$ ). In the present study the pressure losses in the reheaters as well as along connecting pipes from the turbine to these units are neglected; thus,  $P_9 = P_8 = P_7 = P_{10}$ . Finally, the enthalpy at state 10 is determined using both energy and mass balance equations. It is important to remark that the temperature of the superheated steam must be in accordance with the required terminal temperature difference (TTD). The TTD in the present case corresponds to the temperature difference between the temperature of the extracted steam,  $T_2$ , and the temperature of superheated steam,  $T_{10}$ .

### 2.3 The condenser

In the condenser steam from the exhaust of the LP turbine flows on the shell-side while the cooling water circulates inside a network of horizontal tubes. It is apparent that the cooling water that is taken from the Saint-Laurent River changes its mean temperature according to the seasons (summer or winter). For a given water flow rate, the inlet temperature to the condenser determines its operating pressure; thus it is obvious that when this temperature decreases, the condenser pressure also decreases and vice versa. For this reason, the cooling water temperature has a significant effect on the overall plant performance. To perform the present work it is assumed that the inlet water temperature is constant and it is equal to 4°C. Further, the effect of the presence of non-condensable gases in the shell-side of the condenser is negligible. To include their effect necessitates a gas-water dilution model that must take into account the concentration of non-condensable as a function of both pressure and temperature. Therefore, the condenser is modeled as a simple steam-condenser heat exchanger as shown in Figure 4.

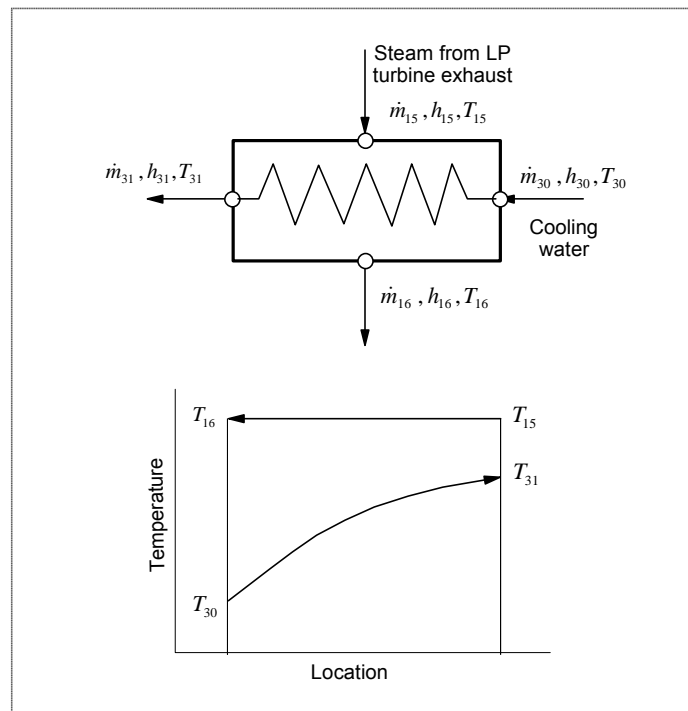


Figure 4 Condenser, simplified model.

A simple energy balance across the condenser, considered ideally adiabatic, yields:

$$Q = \dot{m}_{15}h_{15} - \dot{m}_{16}h_{16} = \dot{m}_{16}(h_{15} - h_{16}), \quad (9)$$

$$Q = \dot{m}_{31}cp(T_{31} - T_{30}), \quad (10)$$

with  $\dot{m}_{31} = \dot{m}_{30}$  and  $\dot{m}_{16} = \dot{m}_{15}$ . The specific water heat capacity ( $cp$ ) is determined at the mean cooling water temperature ( $\bar{T} = \frac{T_{31} + T_{30}}{2}$ ). Combining the energy balance to the heat transfer equation and using an iterative procedure permit to the thermodynamic properties at states 15, 16, 30 and 31 to be determined. To this aim, the heat transfer equation is written as:

$$Q = UA\Delta T_{lm}, \quad (11)$$

where 
$$\Delta T_{lm} = \frac{(T_{16} - T_{30}) - (T_{15} - T_{31})}{Ln \left( \frac{T_{16} - T_{30}}{T_{15} - T_{31}} \right)}$$

The non-availability of all required design data of the condenser leads to the use of some approximations on the overall heat transfer ( $UA$ ). Therefore, it is initially calculated at the operating conditions of the power plant and supposed to be constant.

## 2.4 Feedwater heaters

These types of heat exchangers are modeled based on a modification of the Delaware method commonly used for shell-tube type heat exchanger design [8], generally applied to estimate both heat transfer coefficient and pressure drop in modern feedwater heater units. Most of feedwater heaters are of the three-zone type including superheating, condensing and drain-cooling zones as shown schematically in Figure 5. Instead, the feedwater heater used in the present work is of the two-zone type (i.e., condensing and drain cooling zones).

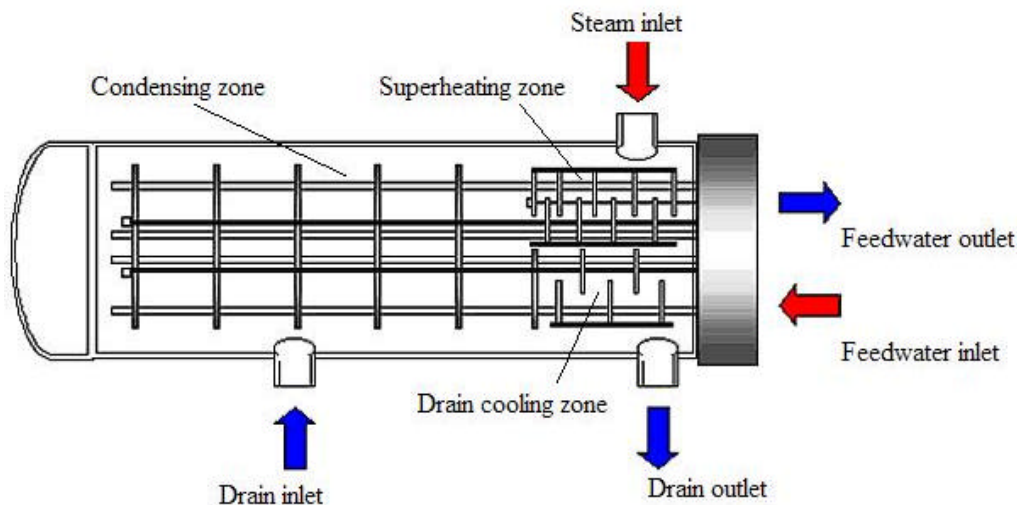


Figure 5 A typical three-zone type feedwater heater.

Flow currents and temperature profiles of a two-zone reheater are illustrated in Figure 6, where the main feedwater mass flow rates are  $\dot{m}_{fwi}$ ,  $\dot{m}_{fwo}$ , the steam mass flow rates are  $\dot{m}_{si}$ ,  $\dot{m}_{so}$  and the mass flow rate of the upstream and downstream drains respectively are  $\dot{m}_{do}$  and  $\dot{m}_{di}$ . Note that to evaluate both the heat transfer and the pressure drop, each zone of the feedwater heater is treated as a separate heat exchanger. The overall heat transfer coefficient is calculated as:

$$(U) = \frac{1}{R_s + R_t + R_w + R_{fo}}, \quad (12)$$

where  $R_{fo}$  is the fouling resistance,  $R_w$  is the tube wall conduction resistance,  $R_t$  is the tube-side convective heat transfer resistance,  $R_s$  is the shell-side convective heat transfer resistance.

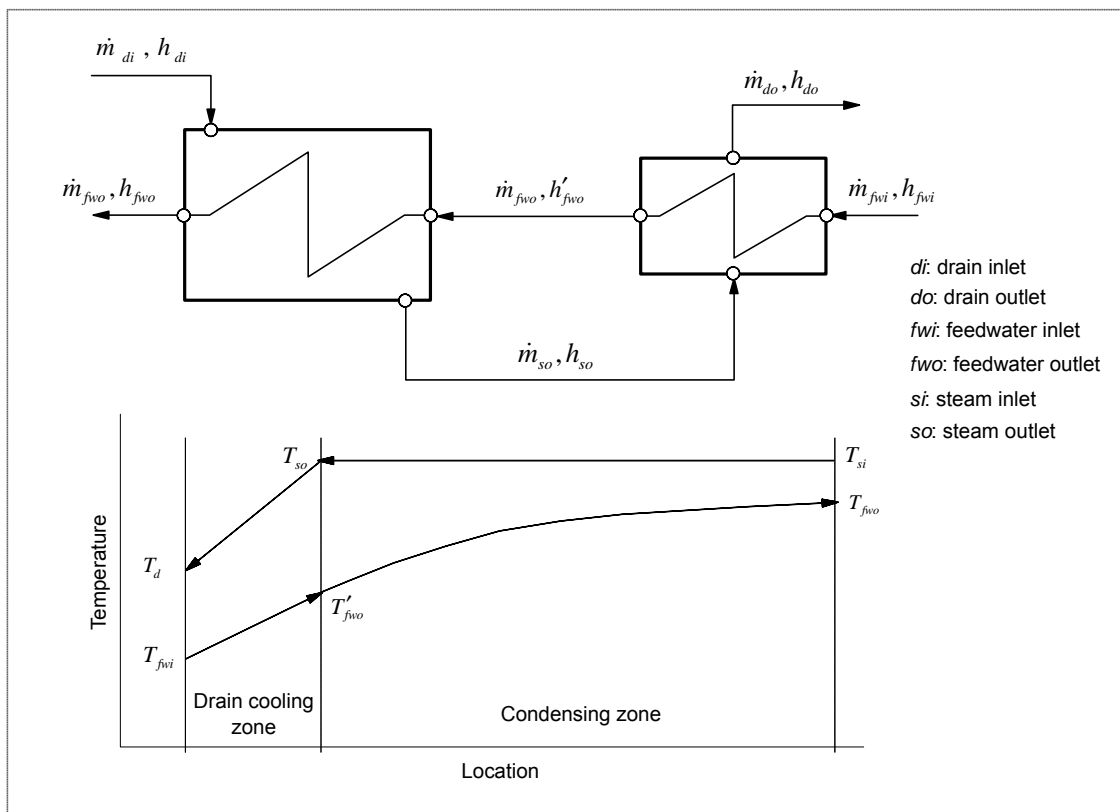


Figure 6 Flow diagram and temperature profiles of a two-zone feedwater heater.

The shell-side pressure drop in the condensing zone is neglected (i.e., it is assumed equal to zero). The application of Delaware method [8] to determine the pressure drop in the steam-side is based on the evaluation of two pressure losses that are then summed up over the entire zone-length; thus:

$$\Delta P_s = ((N_b - 1)\Delta P_b J_b + N_b \Delta P_w) J_l + 2\Delta P_b J_b J_s, \quad (13)$$

where  $J_l$ ,  $J_b$  and  $J_s$  are correction factors to account for leakage, bypass and baffle spacing effects respectively, and  $N_b$  is the number of baffle plates. The pressure drops  $\Delta P_w$  and  $\Delta P_b$  are respectively the pressure drop in one baffle window section and in one cross-flow section, by assuming that there

are no flow leakage or bypass. The determination of  $\Delta P_w$  and  $\Delta P_b$  requires the knowledge of the design parameters provided by the manufacturer. Readers interested in these kinds of calculations are referred to the paper of Weber et al. [9].

After the heat transfer and pressure drop of each zone have been obtained, the next step consists of evaluating the feedwater outlet temperature. It must be pointed out, however, that in a power station having multiple feedwater heaters connected in cascade, the outlet condensate of a heater ( $\dot{m}_{do}, h_{do}$ ) is sent to the inlet of an upstream heater in the feedwater flow path (see Figure 1). The drain inlet ( $\dot{m}_{di}, h_{di}$ ) from an upstream heater flows into the condensing zone and it mixes with the condensate already prevailing in the heater while it flows along the drain cooling zone. Therefore, the calculation of the feedwater outlet temperature starts at the drain-cooling zone where the feedwater flows initially, as it enters into the heater. The equations used to model the drain-cooling zone are given as:

$$Q_{DC} = \dot{m}_s (h_{so} - h_{fwi}), \quad (14)$$

$$Q_{DC} = \dot{m}_{fw} (h'_{fwo} - h_{fwi}), \quad (15)$$

$$Q_{DC} = (UA)_{DC} \Delta T_{lm}, \quad (16)$$

where  $\Delta T_{lm} = \frac{(T_{so} - T'_{fwo}) - (T_d - T_{fwi})}{\text{Ln} \frac{(T_{so} - T'_{fwo})}{(T_d - T_{fwi})}}$ . An iterative procedure is used to carry out, initially, the

calculations in the drain-cooling zone. After satisfying a convenient convergence criterion, the condensing zone is then treated by using the following equations:

$$Q_C = \dot{m}_s (h_{so} - h_{si}), \quad (17)$$

$$Q_C = \dot{m}_{fw} (h_{fwo} - h'_{fwo}), \quad (18)$$

$$Q_C = (UA)_C \Delta T_{lm}, \quad (19)$$

with the logarithmic mean temperature written as:  $\Delta T_{lm} = \frac{(T_{so} - T'_{fwo}) - (T_{si} - T_{fwo})}{\text{Ln} \frac{(T_{so} - T'_{fwo})}{(T_{si} - T_{fwo})}}$ .

The iterative procedure starts with initial guessed temperature values. The difference between the heat transferred in the reheater obtained from the energy balance and the heat transfer equation allows the feasibility of the initial guests to be validated.

## 2.5 The deaerator

The deaerator is used in a power plant to remove incondensable gases dissolved in the feedwater before its return in the boiler or the SGs; thus, preventing corrosion, improving pressure system control and reducing superfluous condensate subcooling in the condenser. Within this thermal unit, the feedwater is

sprayed in thin films or fine droplets into a relatively low-pressure steam atmosphere allowing it to become heated up to saturation conditions. Since the concentration of gas in water is inversely proportional to temperature and directly proportional to pressure, this process permits the amount of non-condensable gases to be significantly reduced. The main problem in the deaerator consists of determining the steam mass flow rate required to heat the inlet water up to the temperature needed, for a given pressure, to reduce the content of dissolved gases. Since these two variables are not necessarily known, it is assumed that they are constant and they correspond to the local steam saturation conditions. Thus, in this work the deaerator is modeled as a direct contact heat exchanger according to the nomenclature given in Figure 7.

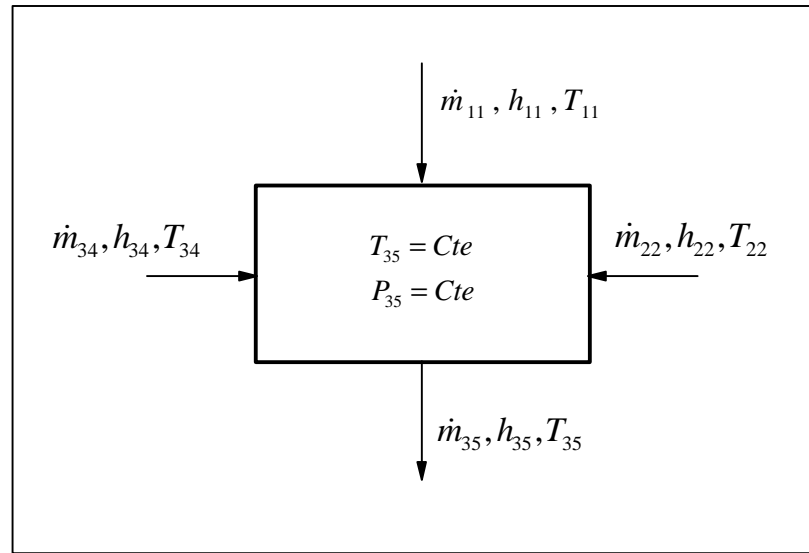


Figure 7 Schematic of the deaerator model.

The operating pressure of the deaerator ( $P_{35}$ ) is then fixed and consequently it determines the saturation temperature at which the feedwater must be heated. The heat/mass balance equation yields:

$$\dot{m}_{22}h_{22} + \dot{m}_{11}h_{11} + \dot{m}_{34}h_{34} = \dot{m}_{35}h_{35}, \quad (20)$$

where  $\dot{m}_{35} = \dot{m}_{11} + \dot{m}_{22} + \dot{m}_{34}$ , and the required steam mass flow rate is then calculated as:

$$\dot{m}_{11} = \frac{(\dot{m}_{11} + \dot{m}_{22} + \dot{m}_{34})h_{35} - \dot{m}_{22}h_{22} - \dot{m}_{34}h_{34}}{h_{11}}. \quad (21)$$

### 3. Simulation-optimization scheme

As already mentioned, the simulation-based optimization combines two software tools: a plant simulator and the optimizer. For a given set of plant parameters, the simulator is invoked to evaluate both the behavior of the system, in terms of thermodynamic states, and the objective function subjected to the constraints imposed by the optimization problem itself. The simulation has been developed using Matlab (version R2007b [10]) with a library for the thermodynamic properties of water and steam (XSteam for Matlab [11]). The optimizer has been written using the Microsoft Visual Basic for

Applications (VBA) programming language. Furthermore, a simulator-optimizer communication interface is carried out via the Windows Dynamic Data Exchange (DDE) protocol. Thus, the simulator, used as client, is responsible to initiate the communication with the VBA application, which in turn acts as server. Figure 8 illustrates the principle of the simulation-based optimization scheme.

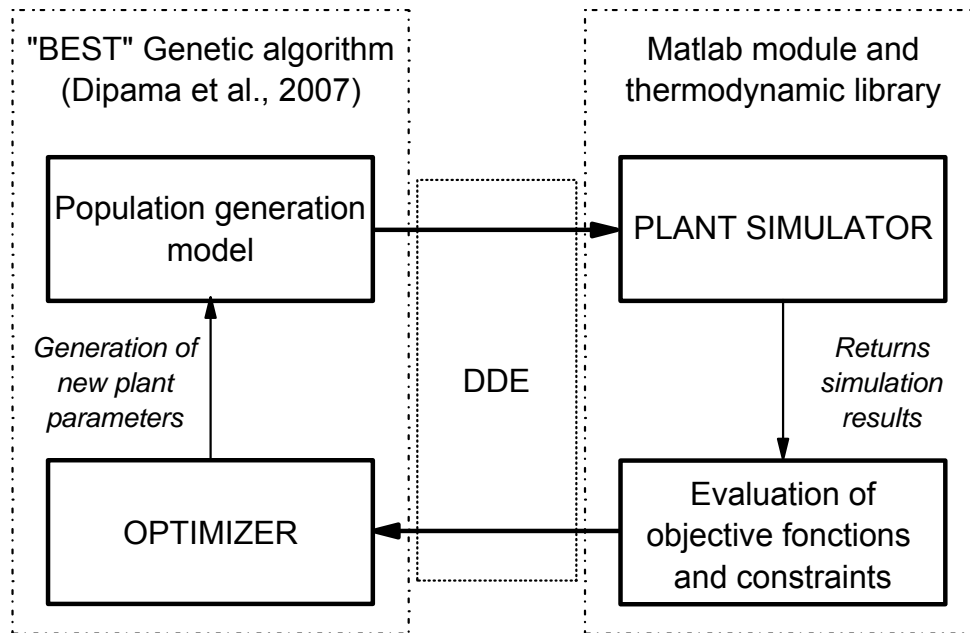


Figure 8 Simulation-based optimization scheme.

The simulator initiates the communication by defining the number of individuals and the number of generations (i.e., chromosomes and population respectively, required by the genetic algorithm implemented inside the optimizer). The optimizer generates the population of potential individuals to be processed by the simulator. After the simulator has evaluated each individual (i.e., possible solution of the problem), the results are then sent again to the optimizer who select the best individuals according to objective functions and constraints imposed to the problem. Then, the best individuals are used to reproduce a new population, with the hope that the new one should be more efficient. This population is once again treated in the simulator and the process is repeated until a given maximum number of generations is completed. Even though, this stop criterion does not necessarily correspond to the convergence of the whole process, we have shown [5,6] that after a given number of generations an accepted global convergence is achieved. Along the present work, we have observed that after 200 iterations Pareto's front does not change; thus, this condition permitted this number to be used as a convenient stop criterion.

#### 4. Results and analysis

The simulation-based optimization was carried out using the "BEST" algorithm [1,5] with a population of 200 individuals. It must be pointed out that in genetic algorithms each individual corresponds to a possible solution of the problem, while the population represents the whole solution-space. Similar to other optimization techniques, it is quite difficult to apply a conventional convergence criterion, therefore 200 iterations were used for each calculation. Further, as already mentioned, the Gentilly-2 simulation software now includes models of most of the major thermal equipments encountered in the power plant. These models necessitate internal iterations to be performed (i.e, feedwater reheaters and

condenser); thus, a unique convergence criterion of  $10^{-4}$  was always satisfied. However, the present scheme does not include external iterations of the whole plant. This particular procedure that will be considered in a future work, will permit local parametric changes associated to the internal simulation of each thermal equipments to be taken into account during plant thermodynamic cycle calculations.

The best tradeoff solutions found during the optimization process are represented by the Pareto's front shown by open circles in Figure 9. These values correspond to the total output mechanical power generated by the turbine (i.e., it includes the power required by the auxiliaries) vs. the overall thermodynamic cycle efficiency, for different operating conditions of the plant. Note that these conditions are randomly determined by the optimizer and they are then used by the simulator to establish the thermodynamic state of the system (see Figure 8). Therefore, Figure 9 does not show the consumption of thermal power by the cycle, which changes along the optimization process. Thus, it can explain the decreasing in efficiency values with increasing the turbine power that forms the Pareto's front. The actual operating condition of the power plant is represented at the bottom left side of the same figure. A comparison of the actual operation of G2 with the solutions that belongs to the Pareto front shows that there are optimal thermodynamic states under which the nuclear power plant can operate, just by conveniently selecting the best combinations of steam extractions values. It is important to remark that for the present optimization only the steam extractions (see Figure 1) were considered as controlling variables.

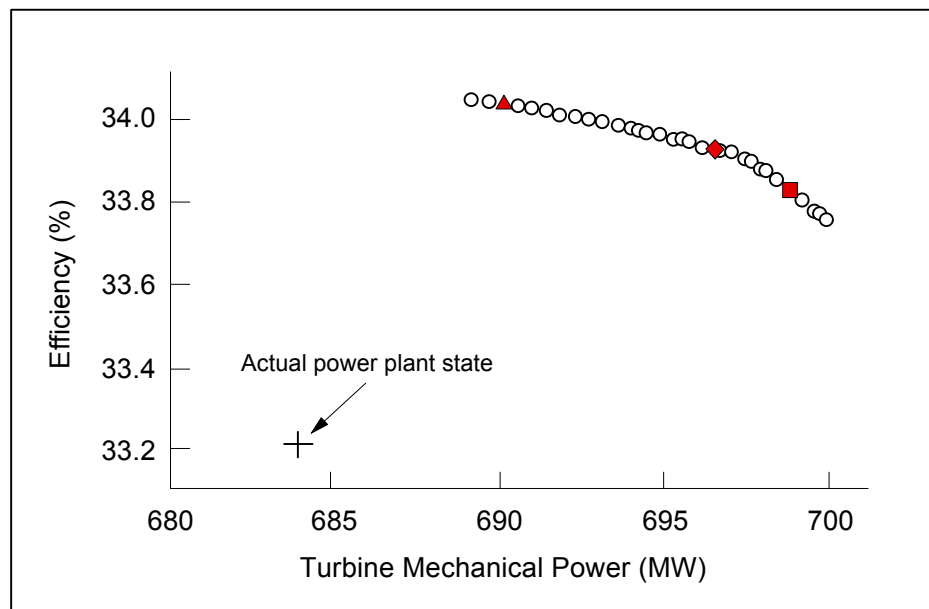


Figure 9 Best tradeoff power plant solutions – Pareto's front.

Figure 10 shows the population of six steam-extraction points, noted as  $y_i$ , which represents some of the optimization variables. Each point in these figures corresponds to individuals that allow best tradeoff solutions to be obtained; thus, they belong to the optimal Pareto's front shown in Figure 9. Figure 10 compares optimal extraction values with the corresponding actual plant operating condition one, shown as dashed lines. The three highlighted points have been arbitrary selected in the population and they are shown using the same symbols in the Pareto's front of Figure 9. In general, it can be observed (Figure 10) that the optimal values of the extractions can be lower or higher than the values of the plant. It is interesting to note that optimal extractions  $y_{11}$ ,  $y_{12}$  and  $y_{14}$  (Figs. 10 c, d and f) do not change during the optimization process, however, they are different to the actual power plant

thermodynamic state. In addition, the implementation of thermal equipment models within the overall optimization procedure modifies local thermodynamic state parameters such as pressure and temperatures. Due to the large amount of information, it is obvious that their comparison with actual operating values becomes quite cumbersome. In turn, care should be taken to validate them among plant design values that could be critical to operate safely some of the major components (e.g., thermal expansion tolerances in the turbine, maximum allowable condensate level inside feedwater reheaters, maximum permitted pressure in the deaerator, etc.). In general, the results given in Figure 10, clearly demonstrate that a convenient combination of steam-extractions can permit a better operation of the Gentilly-2 nuclear power plant.

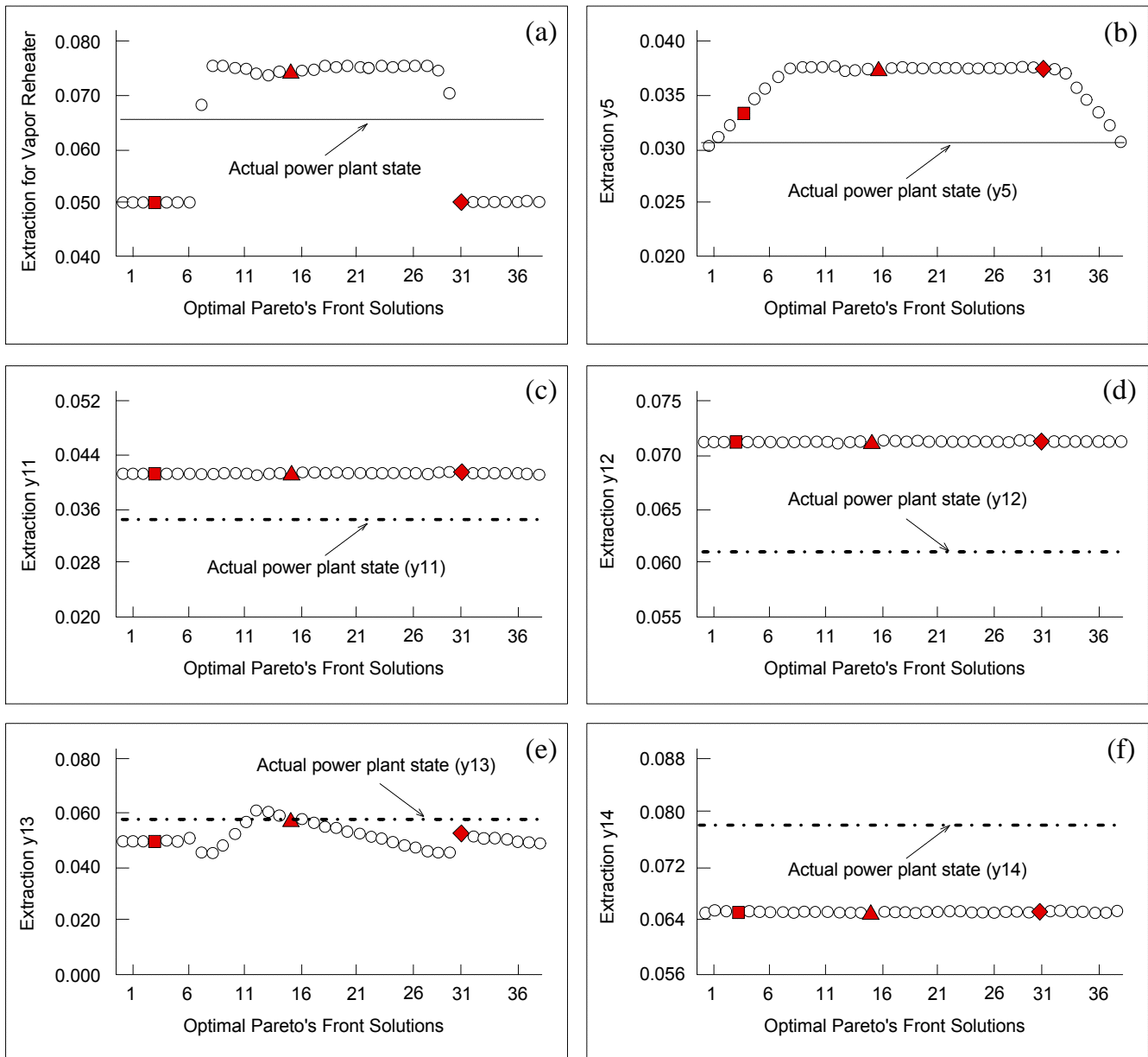


Figure 10 Comparison of optimized steam extractions with actual plant state values.

## 5. Conclusions

To model the secondary loop of G2, several assumptions have been introduced because it was impossible to obtain all necessary data of the power plant. Therefore, the thermodynamic simulation of the power station based on variables provided by Hydro-Quebec does not reproduce exactly the same results observed by plant operators. Thus, the nominal power of G2 obtained from our simulation is 683.85 MW and the thermal efficiency is about 33.20%, comparatively to the results provided by Hydro-Quebec that are 675 MW and 32.8% respectively. In turn, the Pareto optimal solutions obtained by the optimizer are ranging from 689.0 MW to up to 699.8 MW, with cycle efficiencies ranging from 33.8% to 34.0%. These results show clearly that there is a great deal of potential in using the present combined simulation-optimization approach. This work permitted us to determine a set of better trade-off operating conditions of the secondary loop, providing a better and more realistic support to operate the nuclear power plant. Additional work, however, is still required to include extraction pressure losses and to improve the deaerator model.

## 7. References

- [1] W. HOUNKONNOU, J. DIPAMA, F. AUBE & A. TEYSSEDOU, "Multi-objective optimization of thermodynamic power cycles using an evolutionary algorithm," Proceedings of the 29<sup>th</sup> Annual Conference of the Canadian Nuclear Society, Toronto, Ontario, Canada, 2008 May 1-4
- [2] N.R. LIOR, "Energy, exergy, and thermoeconomic analysis of the effects of superheating fossil-fuel in nuclear power plants," *Energy Conversion and Management*, vol. 38, 1997, pp. 1585-1593.
- [3] W.F. SACCO, C.M.N.A. PEREIRA, P.P.M. SOARES & R. SCHIRRU, "Genetic algorithms applied to turbine extraction optimization of a pressurized-water reactor," *Applied Energy*, vol. 73, No.3, 2002, pp. 217-222.
- [4] D.E. GOLDBERG, "Genetic algorithms in search, optimization, and machine learning," Reading, MA. Addison-Wesley, 1989.
- [5] J. DIPAMA, F. AUBÉ, & A. TEYSSEDOU, « Optimisation multi-objectif d'un système de cogénération à l'aide de l'algorithme évolutif BEST », VIII<sup>ème</sup> Colloque Interuniversitaire Franco-Québécois sur la Thermique des Systèmes, Montréal, Québec, Canada, 28-30 Mai 2007.
- [6] J. DIPAMA, A. TEYSSEDOU, & M. SORIN, "Synthesis of heat exchanger networks using genetic algorithms," *Applied Thermal Engineering*, vol. 28, No. 14-15, 2008, pp. 1763-1773.
- [7] A. STODOLA, "Steam and Gas Turbine," vol. 1, 1927, McGraw-Hill.
- [8] K.J. BELL, "Delaware method for shell-side design," In: J.W. Palen (Ed.), *Heat Exchanger Sourcebook*, 1986, Hemisphere Publishing Corp., New-York.

- [9] G. E. WEBER, and W.M. WOREK, "Evaluating the design performance of a feedwater heater with a short drain cooler, Part 1 - Method development," *ASME Journal of Engineering for Gas Turbine and Power*, Vol. 116, No. 2, 1994, pp. 434-441.
  
- [10] MATHWORKS "Matlab support," In: Site of Mathworks [online] [www.mathworks.com](http://www.mathworks.com), (consulted on January 2009)
  
- [11] M. HOLMGREN, "X Steam for Matlab," In: Site of Excel Engineering [online] [www.x-eng.com](http://www.x-eng.com) (consulted on January 2009).

### **Acknowledgments**

This work was funded by the Hydro-Québec chair in nuclear engineering, CANMET (NRCan) and by the NSERC discovery grant # RGPIN 41929.